Cardiotoxicity of acetogenins from *Persea americana* occurs through the mitochondrial permeability transition pore and caspase-dependent apoptosis pathways

**Christian Silva-Platas · Noemí García ·
Evaristo Fernández-Sada · Daniel Dávila ·
Carmen Hernández-Brenes · Dariana Rodríguez ·
Gerardo García-Rivas**

Abstract Acetogenins are cell-membrane permeable, naturally occurring secondary metabolites of plants such as *Annonaceae, Lauraceae* and other related phylogenic families. They belong to the chemical derivatives of polyketides, which are synthesized from fatty acid precursors. Although acetogenins have displayed diverse biological activities, the anti-proliferative effect on human cancer cells has been widely reported. Acetogenins are inhibitors of complex I in the electron transport chain therefore they interrupt ATP synthesis in mitochondria. We tested a new acetogenins-enriched extract from the seed of *Persea americana* in order to investigate if any toxicity was induced on cardiac tissue and determine the involved mechanism. In isolated perfused heart we found that contractility was completely inhibited at an accumulative dose of 77 µg/ml. In isolated cardiomyocytes, the acetogenins-enriched extract induced apoptosis through the activation of the intrinsic pathway at 43 µg/ml. In isolated mitochondria, it inhibited complex I activity on NADH-linked respiration, as would be expected, but also induced permeability transition on succinate-linked respiration. Cyclosporine A, a known blocker of permeability transition, significantly prevented the permeability transition triggered by the acetogenins-enriched extract. In addition, our acetogenins-enriched extract inhibited ADP/ATP exchange, suggesting that an important element in phosphate or adenylate transport was affected. In this manner we suggest that acetogenins-enriched extract from *Persea americana* could directly modulate permeability transition, an entity not yet associated with the acetogenins' direct effects, resulting in cardiotoxicity.

Keywords Mitochondria · Permeability transition · Acetogenins · Avocado · Toxicity

C. Silva-Platas · N. García · E. Fernández-Sada · D. Dávila ·
D. Rodríguez · G. García-Rivas
Cátedra de Cardiología y Medicina Vascular, Escuela de Medicina,
Tecnológico de Monterrey,
Morones Prieto 3000 Pte. CITES. 3er Nivel,
64710 Monterrey, Nuevo León, México

C. Silva-Platas · N. García · C. Hernández-Brenes ·
G. García-Rivas (✉)
Centro de Investigación Básica y Transferencia,
Instituto de Cardiología y Medicina Vascular,
Tec Salud del Sistema Tecnológico de Monterrey,
Monterrey, México
e-mail: gdejesus@itesm.mx

C. Hernández-Brenes · D. Rodríguez
Departamento de Biotecnología y Alimentos,
Escuela de Biotecnología e Ingeniería de Alimentos,
Tecnológico de Monterrey,
Monterrey, México

Introduction

Acetogenins (AGs) are naturally occurring secondary metabolites of plants derived from lipid synthesis, and their distribution is thought to be restricted to the *Annonaceae and Lauraceae* families due to their close phylogenic relationships (Rodriguez-Saona et al. 1998). Although diverse biological activities have been reported, the antiproliferative effect from *Annonaceous* AGs has been extensively described in human cancer cells and murine models of leukemia, and ovarian and breast cancer xenografts (Jolad et al. 1982; Ahammadsahib et al. 1993). The cytotoxic action of AGs probably arises from the strong inhibitory effects on mitochondrial electron transport,

specifically its action on complex I (Degli Esposti et al. 1994). Degli Esposti et al. demonstrated, in bovine cardiac mitochondria, that AGs inhibit the NADH-ubiquinone reductase (complex I), and that bullatacin blocked the proton pumping function of complex I with similar efficiency as rotenone and piericidin. Because of its ability to inhibit the mitochondrial complex I, the main gate of the energy production in the cells, AGs have been considered as candidates for antitumor drugs. Besides blocking complex I in the electron transport chain, AGs are also potent inhibitors of the NADH oxidases particular to the plasma membranes of tumor cells (Morré et al. 1995). Both mechanisms of action result in the inhibition of ATP production and may account for the effectiveness of AGs in killing multiple-drug resistant tumors.

Mitochondrial permeability transition (mPT) can lead to cell death, and can be induced by inhibition of respiratory chain complexes, high intracellular Ca^{2+}, reactive oxygen species (ROS), or proapoptotic proteins such as Bax; whereas it is inhibited by cyclosporine A (CsA), bongkrekic acid (BKA) or Bcl-2 (Gustafsson and Gottlieb 2007; Halestrap 2009). The opening of large inner membrane pores causes equilibration of ions within the matrix and the cytosol, dissipating the membrane potential ($\Delta\Psi$) and uncoupling the respiratory chain. The volume deregulation following the opening of the permeability transition pore results in swelling of the matrix, leading to outer membrane disruption and the release of cytochrome c and other caspase-activating proteins into the cytosol, ultimately resulting in apoptosis of the cell (Liu et al. 1996). In this regard, the anti-proliferative mechanism of AGs, Yuan et al. found that annonacin could arrest T24 bladder cancer cells at the G1 phase and cause cytotoxicity in a Bax- and caspase-3-related pathway (Yuan et al. 2003). In addition, persin from avocado (Persea americana, a representative of Lauraceae family) induced apoptosis in human breast cancer cells independently of the p53, estrogen receptor, and Bcl-2 status of the cells, but did cause the release of cytochrome c and Smac/DIABLO into the cytoplasm, significantly attenuated blocking of the Bim pathway (Oelrichs et al. 1995).

On the other hand, an extract from Annona muricata, also enriched with AGs, caused a significant decrease in body weight, abnormal neuronal function, and death in rats. This finding correlates with the ethno-pharmacological observation about the similar side effects of AGs and a neurodegenerative tauopathy, which was supposedly linked to the consumption of Annonaceous plants (Caparros-Lefebvre and Elbaz 1999; Champy et al. 2003). Escobar-Khondiker et al. further found that annonacin induced the retrograde transport of mitochondria to decrease ATP levels, which changes the energetic homeostasis similar to some neurodegenerative diseases and heart failure (Escobar-Khondiker et al. 2007; Neubauer 2007). The possible adverse effect of AGs on neurons and cardiac cells should be a concern in advanced pharmaceutical applications for alternative therapy. In this study, we investigated an AGs enriched extract (AGE) from Persea americana seeds, and explored various mechanisms that might be responsible for its toxicity. We found that the cardiac function of isolated rat heart was completely depressed, impairing relaxation and heart rate. Toxicity in adult rat cardiomyocytes was mediated by caspase activation and not necrosis. Our results further suggest that the toxicity of AGE is related to the inhibition of complex I and opening of the permeability transition pore, which leads to the leaking of important metabolic and pro-apoptotic components.

Materials and methods

Source of Hass avocado seeds

Avocados seeds (Persea americana Mill, cv. Hass) used in the study were obtained from a local market. Mature Hass avocados were selected for the experiments based on their skin appearance (complete change from green to black), fruit palpability (slightly yield to gentle pressure) and flesh appearance (green/yellowish rich creamy flesh with no black spots). Seeds were stored at -80 °C until AGs extraction. Equal weight (50 g each) seeds were combined, homogenized, and extracted immediately.

Extraction

Avocado seeds were crushed using a colloidal mill to obtain particles with an average radius of 0.5–2 mm. These particles were mixed with acetone (ratio of 1:2,w/v) and stored at 25 °C for 24 h in order to obtain a raw avocado seed extract. This extract was concentrated using a rotary evaporator (35 °C, 22) to obtain a reddish extract (1.86 g). The raw extract was partitioned using a non-miscible solvent system comprised of 100 ml of heptane (upper phase) and 100 ml of methanol (lower phase), obtaining an upper fraction with the less polar compounds, an interphase, and a lower fraction with the polar compounds. The collected lower fraction was concentrated using a rotary evaporator and further partitioned in a non-miscible solvent system comprised of 100 ml of ethyl acetate (upper phase) and 100 ml of water (lower phase) to yield 0.52 g of the ethyl acetate soluble fraction.

HPLC profiling for AGs in extracts

The chromatographic profiles of the extracts were obtained as described by Yang et al. (Yang et al. 2009), with some modifications. The extracts were dissolved in isopropanol.

An Agilent 1100 Series High Performance Liquid Chromatographer (HPLC), with a DAD G1315B diode array detector, a G1329A autosampler, and G1312A binary pump was used. The injected sample volume was 2 μl. The separation was achieved in reverse phase using a Zorbax Extended-C18 (100×3 mm d.i., 3.5 μm) column. The detector was set to 220 nm wavelength. The mobile phase consisted of 100 % water as phase A and 100 % methanol as phase B. The solvent gradient was set at a 0.25 ml/min flow rate, starting with 50 % B, followed by 80 % B from min 15–30, 83%B at min 45, 93%B at min 60, 65%B at min 65 and 100%B from 75 to 80, with a post-time of 8 min. The quantification of the obtained fractions after partitions was performed by external calibration in triplicate using persenone A (purified in our laboratory from avocado seed) as standard. The results were expressed in mg of persenone A equivalents per mg of fraction (on dry weight basis). Chromatographic profiles indicated that the ethyl acetate fraction contained a concentration of AGs with a purity of ~55 %, yielding 0.554 mg of persenone A equivalents per mg of fraction. The AGE used in further studies was prepared by adjusting 100 μg of fraction/ml (AGE).

Animal use

All the experiments were performed in accordance to the animal care guidelines of the Guide for the Care and Use of Laboratory Animals published by the US National Institutes of Health (NIH Publication No. 85–23, revised 1996). All procedures were approved by the animal use and care committee of the Tecnológico de Monterrey Medical School.

Isolated perfused heart experiments

Weanling male Wistar rats (250–300 g) were used. Heparin was injected (10^3 IU/Kg, i.p.) 20 min prior to anesthesia with pentobarbital (100 mg/Kg, i.p.). Once the corneal reflex was absent bilaterally, the heart was excised through an abdominal approach. The ascending aorta was visualized and cut. The time from cutting the diaphragm to placing the heart in a cardioplegic solution was less than 60 s to avoid ischemia. The hearts were mounted in accordance with the Langendorff model and perfused with Krebs-Henseleit buffer ((in mM) NaCl 125, KCl 5.4, $MgCl_2$ 1.0, NaH_2PO_4 0.5, $NaHCO_3$ 25, $CaCl_2$ 2.5, glucose 11, and octanoate 0.1) as previously described (De Jesús García-Rivas et al. 2005). Once autonomous contraction was established, a latex balloon connected to a pressure transducer was inserted into the left ventricle; the balloon was filled with saline solution. To obtain an iso-volumetrically beating preparation, a latex balloon filled with saline solution and connected by a catheter to a transducer (FOBS-28. WPI)

was inserted into the left ventricle and inflated to provide an end-diastolic pressure between 15 and 20 mm Hg. Before each experimental protocol was initiated, the isolated hearts were set at a mean arterial pressure of 60 mm Hg and were allowed to stabilize for 10–15 min. Data Trax software (WPI. Sarasota. Florida) was used for continuous recording of heart rate, left ventricular pressure (LVP), and maximum positive and negative derivative of left ventricular pressure (±dP/dt) throughout the experiments. Baseline was established during 10 min of K-H perfusion. Each concentration of AGE was allowed to act on the heart for 10 min. Hearts in the control group were perfused with AGE vehicle (ethanol) during the whole experimental time.

Cardiomyocytes experiments

Rat ventricular myocytes were isolated by collagenase II digestion of perfused hearts using the modified method of Wolska and Solaro (Wolska and Solaro 1996). Rats were heparinized and anesthetized by peritoneal injection (10^3 IU/Kg and 100 mg/kg, respectively) before removal and hanging of the heart. Cells were suspended in Tyrode solution ((in mM): 130 NaCl, 5.4 KCl, 0.4 NaH_2PO_4, 0.5 $MgCl_2$, 1 $CaCl_2$, 25 HEPES, 22 glucose, pH 7.4, with NaOH). The cell pellet was suspended in Dulbecco's Modified Eagle Medium (DMEM): fetal calf serum (2 %), penicillin (100 U/ml) and streptomycin (100 μg/ml). The suspension enriched with non-adhesive myocytes was transferred to collagen-coated culture dishes at a density of 10^4 cells per cm^2. The cells were incubated at 37 °C in 95 % air and 5 % CO_2 for 12 h prior to all experiments. After this time, the medium was added with varying concentrations of AGEs (0–10^3 μg/ml) and the incubation was continued for 4 h. At the end of the incubation period, we determined the cytotoxicity of AGEs using the Alamar Blue viability test (Gibco, USA). Release of cytoplasmic lactate dehydrogenase (LDH) was determined using CytoTox-ONE homogeneous membrane integrity kit from Promega (Madison, WI). The fluorescent signal was measured with an excitation wavelength of 560 nm and an emission wavelength of 590 nm. The LDH release is expressed as percentage of total LDH (i.e., following complete lysis of cells). The activity of caspases 3 and 7 was measured in cell pellets using Apo-ONE fluorescent substrate (Promega, USA). Caspase 8 and 9 activity was determined after 1.5 h of exposure to AGE using CaspaseGlow9 and CaspaseGlow8 (Promega, USA).

Isolated mitochondria experiments

Heart tissue from the left ventricle was minced and homogenized in isolation medium, containing ((in mM) 125 KCl, 1ethylenediaminetetraacetic acid, and 10 N-2-hydroxyl piperazine-N0-2-ethane sulphonic acid (10 HEPES)- HCl,

pH 7.3). The mitochondrial fraction was obtained by differential centrifugation using the protease Nagarse, as previously described (de Garcia-Rivas et al. 2006). Mitochondrial oxygen consumption was measured using a Clark-type oxygen electrode. The experiments were carried out in 0.5 ml of assay medium, containing ((in mM) 125 KCl, 10 HEPES-HCl and 3 KH_2PO_4-TRIS, pH 7.3). State 4 respiration was evaluated in the presence of 10 mM succinate plus 1 μg/ml rotenone, or 5 mM, glutamate-malate. CCCP-stimulated respiration was determined in the presence of 0.08 μM of carbonyl cyanide m-chlorophenyl hydrazone (CCCP). State 3 respiration was measured after addition of 200 μM ADP. The membrane potential was measured by fluorometry using 5 μM safranine (Waldmeier et al. 2002). Mitochondrial calcium uptake was measured with the metalochromic indicator, Arsenazo III, according to Chavez et al. (Chávez et al. 2003) using 1 mM EGTA, and 0.05 free Ca^{2+}, as calculated by using the Chelator program (Th. Schoenmakers, Nijmegen, the Netherlands), pH 7.3. Protein content was measured by the Lowry method.

Activity of adenine nucleotide translocase (ANT)

The adenine nucleotide translocase activity was measured as previously reported (Ortega 2009). Mitochondrial protein (1 mg) was incubated for 1 min with AGE, then 30 μM [3H] ADP was added (specific activity: 1,300 cpm/nmol) and then an aliquot was filtered through a 0.45-μm pore filter and washed with 0.1 M KCl. The radioactivity retained in the filter was measured in a scintillation counter.

Oxidative Stress measurements

Mitochondrial aconitase activity [E.C.4.2.1.3] was determined with spectrophotometry by monitoring the $NADP^+$ reduction (340 nm) by isocitrate dehydrogenase [EC 1.1.1.42] upon addition of 1.0 mM sodium citrate, 0.6 mM $MnCl_2$, 0.2 mM $NADP^+$, and 1.0 unit/ml isocitrate dehydrogenase [EC 2.7.11.5], as previously reported (Bulteau et al. 2005). A change in the concentration of H_2O_2 in the medium was detected by fluorescence of the oxidized Amplex Red (Invitrogen, USA) product using excitation and emission wavelengths of 550 and 585 nm, respectively. The response of Amplex Red to H_2O_2 was calibrated by sequential additions of known amounts of H_2O_2 at 100–1,000 pmol/min. Membrane lipid peroxidation was analyzed by measuring the generation of thiobarbituric acid-reactive substances (TBARS) as reported by Ohkawa et al. (Ohkawa et al. 1979) Mitochondrial protein (1 mg) was added to 1 ml of basic medium supplemented with 5 μg rotenone and 50 μM Ca^{2+}; 20 min after incubation, TBARS were extracted with butanol and measured in a spectrophotometer at 532 nm, and their concentration was calculated using a tetraetoxypropane curve.

Chemicals

Collagenase type II was purchased from Worthington (USA), advanced DMEM, fetal bovine serum, and antibiotics from GIBCO (USA), and all the reagents were purchased from Sigma—Aldrich (USA).

Statistical analyses of data

All data are shown as the mean±the standard deviation. When comparing groups for significance, ANOVA test was used. SigmaPlot 10 and SigmaStat 3.1 (Systat Software Inc., Germany) were used for data management and analysis.

Results and discussion

Induction of cardiotoxicity by AGE

To assess the effect of the AGE on the cardiac function, isolated rat hearts were perfused with increasing concentrations of AGE. After AGE was perfused for 10 min, a time-dependent inhibitory effect on mechanical performance was apparent. As shown in Fig. 1 panel A, we observed a dose-dependent inhibition with a half inhibitory concentration (IC_{50}) of 1.3±0.3 μg/ml. AGE depressed heart contractility by increasing the end diastolic ventricle pressure (60 vs 15 mm Hg, Fig. 1b) and lowering the heart rate (4.1 vs 4.8 Hz, Fig. 1c). The developed pressure in the ventricle (dp/dt) was also affected (+1550 vs+2250 $mmHgxs^{-1}$, Fig. 2d). Full inhibition was reached at a dose of 77 μg/ml. To our knowledge, there is no previously published experimental data reporting that AGs can affect ex vivo cardiac function. Interestingly, congestive heart failure and death occured in ostriches and hens ingesting avocado leaves and immature fruit enriched with AGs. The cardiomyopathy was characterized by myocyte infiltration and necrosis (Burger et al. 1993). Next, we examined the AGE cardiotoxicity using Alamar blue on adult rat cardiomyocytes (Fig. 1e). AGE significantly induced a potent cytotoxic activity in a dose-dependent manner (IC_{50} values of 43±4 μg/ml). As previously shown, persin, an AG from avocado, produces a cytotoxic effect on mammary gland, myocardium (Oelrichs et al. 1995) and human breast cancer cell lines at similar dose (≈10 μg/ml) (Butt 2006). At our IC_{50}, we found no difference in the level of release-lactate dehydrogenase, a marker for necrosis (Fig. 1f). Interestingly, a significant increase in the activities of caspases 3 and 7 was observed, with the release of cytochrome c from the mitochondria being one of the major triggers for apoptosis. Cytosolic cytochrome c induces caspase-9-dependent activation of caspase-3 and cleavage of the Poly ADP ribose polymerase involved in DNA repair (Lee and Gustafsson 2009).

Fig. 1 Effect of AGE on isolated perfused rat heart where the heart contractility (**a**) is diminished by AGE. MPI = (left ventricular pressure x heart rate), normalized to basal MPI (%). This effect is a consequence of the decrement in the developed pressure (**b** and **d**) and a lower heart rate (**c**), as seen in the representative recordings after dosing AGE at IC_{50}. Toxicity of AGE on rat heart ventricle myocytes. Cell viability (**e**) showing the half inhibitory dose (IC_{50}) on 10^4 cells/cm^2 after 4 h of treatment with AGE (*White Circle*). Vehicle (*Black Circle*). Comparison of activities (**f**) of proteins used as markers of cell death, caspases 3 & 7 for apoptosis, and lactate dehydrogenase (LDH) for necrosis. 10^4 cells/cm^2 treated 4 h with AGE at LD_{50}. Comparison of activities (**g**) of caspases used as markers of intrinsic, or extrinsic apoptosis initiation during cell death. 10^4 cells/cm^2 treated 1.5 h with AGE at LD_{50}. The values are mean ± S.D. of 7 separate experiments. *$P \leq 0.05$ vs vehicle
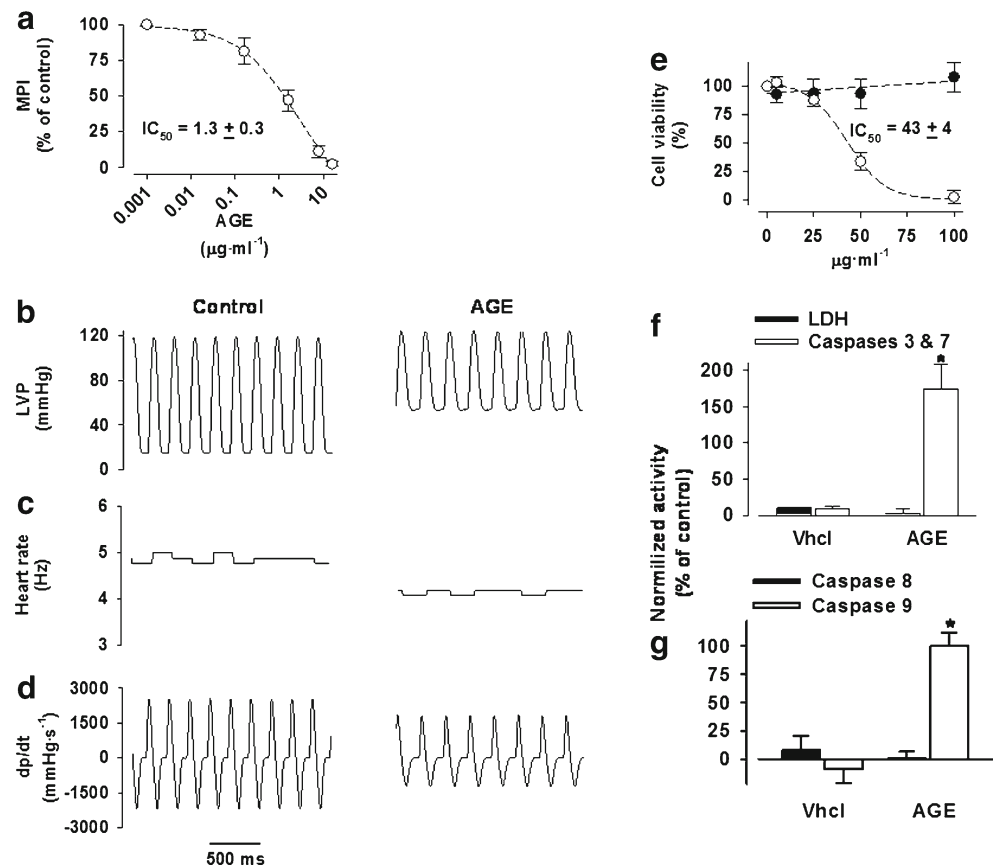
AGE treatment increased the activity of caspase-3 and caspase-7 compared to vehicle-treated cells. However, caspase 8 activity was not enhanced, suggesting that the cell surface receptor pathway is not implicated (Fig. 1g). These results indicated that the mitochondrial pathway was involved in the apoptosis signal pathways induced by AGE. In accordance with our results, previous studies in cancer cells have shown that persin elicits an arrest in the G_2-M phase of the cell cycle and induces a caspase-dependent apoptotic program associated with the release of mitochondrial cytochrome *c*. The latter was dependent on expression of the Bcl-2 protein (Butt 2006; Roberts et al. 2007).

AGE inhibits mitochondria respiratory activity and decrease $\Delta\Psi$

AG compounds are potent inhibitors of the mitochondrial respiratory complex I (NADH—Ubiquinone oxidase reductase, EC: 1.6.5.3) (Ahammadsahib et al. 1993; Degli Esposti et al. 1994; Murai et al. 2006; Alvarez Colom et al. 2009). Thus, we evaluated the effect of AGE on the mitochondrial respiratory chain. As shown in Fig. 2 panel A, we measured the effect of AGE on CCCP-mitochondrial respiration with malate-glutamate as substrates. We observed a dose-dependent inhibition with a half inhibitory concentration (IC_{50})=39±

4 µg/ml. When substrate was changed to succinate, this dose only decreased respiration by 9 %. The failure to inhibit succinate-linked respiration indicates that, similar to the classical electron transport inhibitor rotenone, AG inhibit respiration mainly by altering mitochondrial complex I (Murai et al. 2006). When malate-glutamate was used as substrate, mitochondrial respiration was rapidly and completely inhibited by 130 µg/ml AGE (Fig. 2a). In accordance with reports by several groups, the inhibition of the electron transport chain alters mitochondrial function and induces apoptosis in a variety of cell types (Pastorino et al. 1995; Wolvetang et al. 1994; Isenberg and Klaunig 2000). The inhibition of cell respiration by compounds such as rotenone, has been attributed to the blocking of the oxidation of reduced nicotinamide adenine dinucleotide (NADH) at complex I of the electron transport chain, thus maintaining a high NADH/NAD ratio (Pastorino et al. 1995). This previously findings could be comparable to the mechanism of toxicity elicited by AGE.

At lower AGE concentrations, inhibition of respiration occurs more gradually, taking several minutes to reach completion. This was probably due to a slow uptake of AGE into the mitochondria. The addition of succinate to AGE-treated mitochondria partially reversed the blocking of oxygen consumption seen with malate-glutamate as substrate (data not shown).

AGE showed a significant inhibition on state-4 respiration (without ADP) in NADH-linked respiration (Fig. 2b). However, succinate-linked respiration showed a marked increase in the oxygen consumption rate by 45 to 75 nmol O/min/mg protein, suggesting that AGE acts as a mitochondrial uncoupler (see also Fig. 2b). As expected, the uncoupling effect resulted in a decrease of the respiratory control ratio in succinate-linked respiration (RCR, control value 4±4 to 1.2±0.8). In addition, we observed a significant $\Delta\Psi$ reduction in AGE-treated mitochondria. After AGE addition at 100 µg/ml, the mean fluorescent intensity of safranine decreased 25 % vs. control (Fig. 3b). Mitochondrial uncoupling agents transport protons across the inner mitochondrial membrane (IMM), dissipating the $\Delta\Psi$ required for the coupling between electron transport and oxidative phosphorylation. They are usually weak
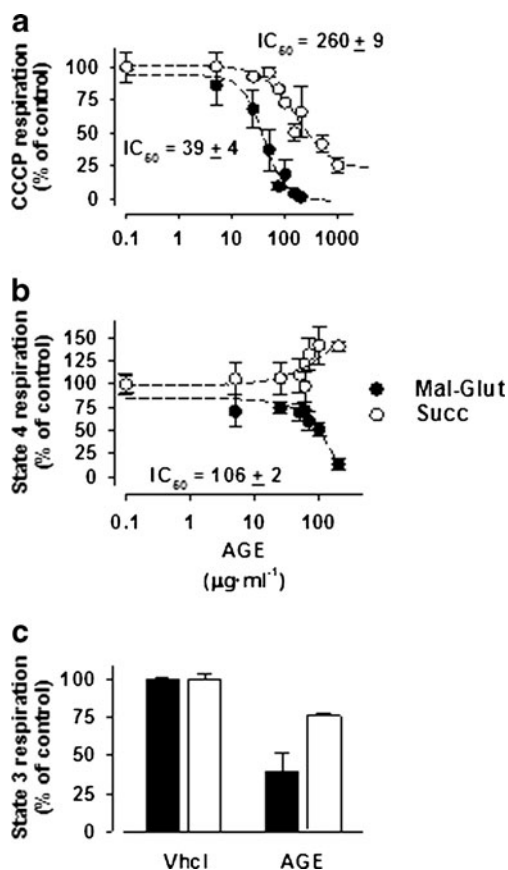

Fig. 2 Inhibition of respiratory activity in isolated rat heart mitochondria. a Effect of AGE on malate-glutamate (Mal-Glut) or succinate (Succ) linked-respiration. Maximal respiration rate was achieved by adding 0.08 µM CCCP. After 20 s, AGE was added and the first minute of oxygen consumption rate was compared. b Effect of AGE on Mal-Glut or Succ linked-respiration. State 4 respiration was established in the absence of ADP. AGE was added and the first minute of oxygen consumption rate was compared. c Effect of AGE on Mal-Glut or Succ dependent respiration. State 3 respiration was established by adding 1 mM ADP. AGE was added and the first minute of oxygen consumption rate was compared. Mitochondria 0.3 mg/ml. The values are mean ± S.D. of 7 separate experiments

organic acids with pKa values ranging from 4 to 7 (Terada 1981). The chemical features that possibly enable persin, persenone A and B to uncouple mitochondria consist of an acidic-dissociable acetyl or carbonyl group with a pKa of 6.5, an electron-withdrawing moiety, and a bulky hydrophobic aliphatic chain. The typical geometric arrangement of this type of structure is considered to be critical for compounds to achieve a strong mitochondrial uncoupling activity (Terada 1981). The aliphatic chain, in association with the double-bond hydroxyl-keto group conjugation in persenone A and B, could stabilize its anionic species through delocalization of the charge over its structure. Consequently, protonated AG may diffuse from the mitochondrial intermembrane space (high H+concentration) into the matrix (low H+concentration), dissociate, and diffuse back in its ionized form to the intermembrane space where it may be protonated again, repeating the cycle. In addition, it has been demonstrated that mitochondrial uncouplers induce apoptosis in several cell types (de Graaf et al. 2004). 2,4 dinitrophenol (DNP) and carbonylcyanide-4-triuoromethoxyphenylhydrazone (CCCP), for example, induced apoptosis by direct action on the mitochondria. These results may indicate that AGE-induced mitochondrial uncoupling causes membrane permeabilization. Apoptosis induction by uncouplers may be via cytochrome c release from the mitochondria into the cytosol followed by activation of caspases.

Loss of permeability of the mitochondrial membrane to protons could occur in situations of extensive and non-specific membrane permeabilization, such as those implicated in the membrane lipid peroxidation as a consequence of ROS accumulation (Castilho et al. 1994). Table 1 shows that lower doses of AGE did not elicit a significant pro-oxidant action on mitochondria during succinate-linked respiration. As expected, the inhibition of the respiratory chain by AGE increased the production of the ROS hydrogen peroxide (H_2O_2) by almost 2 fold (Table 1). Aconitase activity was diminished in this scenario, but still no evident damage was seen on phospholipids of the mitochondrial membrane by TBARS experiments. According to this data, it is evident that there is an increment in ROS production due to the AGE, but seems to be not entirely responsible for the changes in IM permeability, suggesting that there might be a direct role of AGE in mPTP opening.

AGE decreases ANT activity and promotes mitochondria permeability transition

In the resting state, the addition of 100 µg/ml AGE increased the non-phosphorylating respiration (Fig. 2b), which indicates an increase in the H+ conductance across the inner membrane. State 3 respiration, in contrast, was decreased by AGE (Fig. 2c), suggesting that AGE might have
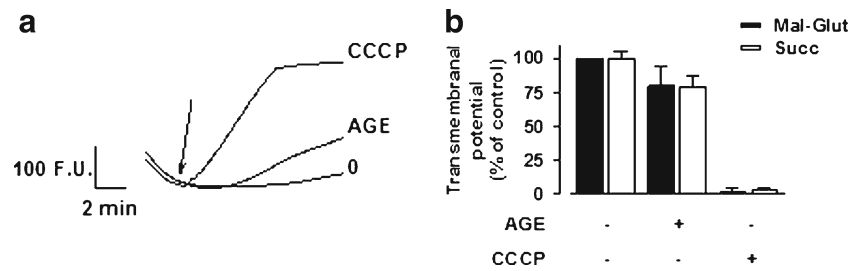
Fig. 3 Effect of AGE on transmembrane potential of mitochondria. **a**. The arrow indicates the addition of 100 µg/ml AGE, or 0.08 µM CCCP. **b** Quantitative representation of maintenance of the transmembrane potential in mitochondria. Complete retention (100 %) was established for vehicle-treated mitochondria. The values are mean±S.D. of 6 separate experiments

additional targets on oxidative phosphorylation components. One of the constituents of the phosphorylative system is the ANT, which is responsible for: (ADP)-ATP translocation that imports ADP to the matrix and exports ATP to the cytosol. To test whether ANT can be modulated by AGE, ADP/ATP exchange experiments were performed. Figure 4a shows the inhibitory property of AGE on the ANT in a dose-dependent manner (IC_{50}=132±1 µg/ml). Such inhibitory effect alters ADP-stimulated respiration (Fig. 2c). At a lower dose (40 µg/ml), ANT activity was diminished by 30 %, indicating that AGE apparently modulates ANT activity.

Moreover, ANT is suggested to be a structural component of the mPT pore (McStay et al. 2002). The mPT pore opening compromises the normal integrity of the mitochondrial inner membrane, resulting in uncoupled oxidative phosphorylation, ATP decay, mitochondrial swelling, and release of apoptogenic factors; indicating a key role for the mPT pore in apoptosis (Gustafsson and Gottlieb 2007). In order to investigate whether AGE was able to induce the mPT, we determined the calcium retention in AGE-treated mitochondria. AGE given in a dose-dependent manner was able to induce mPT pore opening (IC_{50} (µg/ml)=29±5, and 49±4, for malate-glutamate and succinate linked respiration

respectively) (Fig. 4c). Figure 5a shows that AGE-induced mitochondrial Ca^{2+} release in a pathway that was sensitive to the classical mPT inhibitor, CSA. At a lower dose (50 µg/ml), mPTP pore opening was inhibited by 70 % by CSA, however a higher dose was insensitive to CSA. As previously decribed by Crompton et al. (Crompton et al. 1998) matrix cyclophilin D binds to complexes of VDAC and ANT in order to form the mPT pore complex. It has also been reported that CycP-D is more of a regulatory component of the mPT pore than a structural one. Our results suggest, that CSA blocks the AGE-induce mPT pore opening by either direct modulation of ANT or inhibition of CycP-D binding to the ANT.

The opening of the mPT is another event potentially implicated in AGE toxicity on cardiac cells. It has been proposed that the loss of mitochondrial membrane potential due to uncoupling increases the probability of the mPT pore opening due to its voltage-sensitive property (Bernardi 1992). At low membrane potentials, the NAD(P)H transhydrogenase cannot sustain high levels of mitochondrial reducing power, thus favoring Ca^{2+}-induced ROS accumulation, thiol cross-linkage, and mPT pore opening (Vercesi 1987). The sudden increase in MIM permeability enhances colloidal osmotic pressure in the mitochondrial matrix,

Table 1 Oxidative damage in AGE-treated mitochondria. Mitochondrial aconitase activity as measured by NADPH production. Mitochondria (0.3 mg/ml) treated with AGE (50 µg/ml) for 5 min in standard respiration media were centrifuged and washed, followed by suspension in aconitase buffer assay. Hydrogen peroxide (H_2O_2) production as measured with Amplex–Red reagent in presence of HRP. Membrane lipid peroxidation (MDA) as measured by the generation of thiobarbituric acid-reactive substances (TBARS). Mitochondria (0.3 mg/ml) treated with AGE (50 µg/ml) for 5 min in standard respiratory media. The values are mean ± S.D. of 4 separate experiments. *$P \leq 0.05$ vs control group

Oxidative stress marker

| AGE	Trolox	Aconitase activity [nmolNADPH(minxmg)$^{-1}$]		H_2O_2 production (pmolxmg^{-1})		MDA (nmolTBARSxmg^{-1})	
		Mal-Glut	Succ	Mal-Glut	Succ	Mal-Glut	Succ
-	-	35±8	34±7	175±38	85±3	0.40±0.05	0.40±0.08
+	-	24±3*	17±2*	324±25*	195±3*	0.54±0.14	0.40±0.04
+	+	28±8	22±10	255±13*	193±5*	0.42±0.04	0.36±0.04

Fig. 4 Effect of AGE on ANT activity and permeability transition in isolated mitochondria. **a** Exchange of ADP/ATP in mitochondria is inhibited by AGE. Mitochondria 0.3 mg/ml. [^{3}H] ADP 0.03 mM (specific activity 1,300 cpm/nmol). **b** Representative recording of calcium release as indicative of permeability transition. **c** Velocities of calcium release from mitochondria after treatment with AGE. The values are mean±S.D. of 7 separate experiments. *$P \leq 0.05$ vs baseline
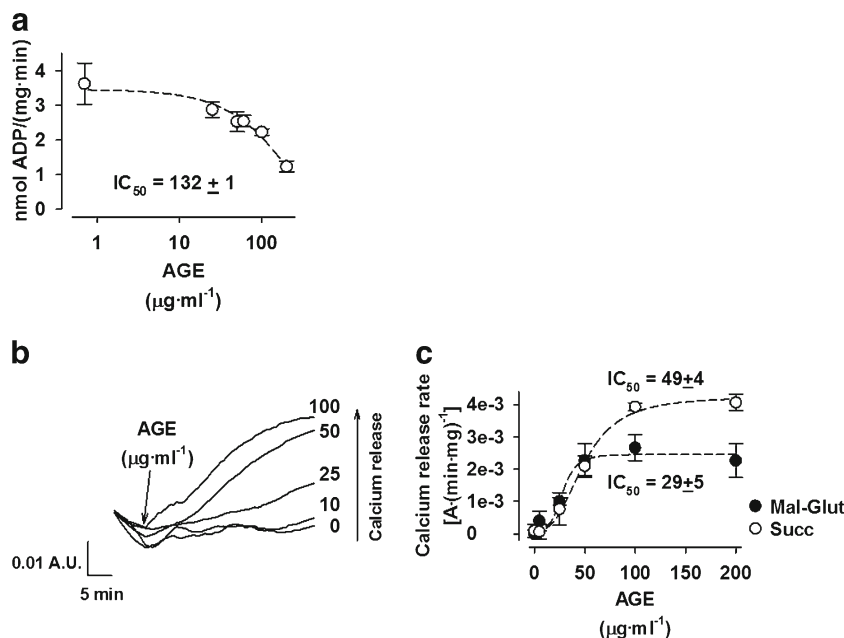
ultimately leading to matrix swelling and rupture of the mitochondrial outer membrane (MOM). Rupture of the MOM releases pro-apoptotic proteins from the mitochondrial intermembrane space to the cytoplasm, and thereby, initiating caspase-dependent apoptosis (Gustafsson and Gottlieb 2007). Permeabilization of the MOM may also occur due to formation of non-selective channels induced by translocation of pro-apoptotic Bcl-2 family proteins to the mitochondria. In this regard the anti-proliferative mechanism of other AGs are associated to the Bax-and caspase-3-related pathway (Yuan et al. 2003; Oelrichs et al. 1995). Due to its central role in lethal functions, the mPT represents a

potential therapeutic target for cell survival. Studies done over 20 years ago have demonstrated that acute cardiac ischemia-reperfusion (IR), which is caused by interruption of substrates and oxygen delivery followed by reoxygenation and substrate supply, is associated with opening of the mPT pore (Arteaga et al. 1992). Furthermore, pharmacological and conditional inhibition of the mPT pore formation significantly improved cardiac function by reducing ischemic injury and myocardial infarct size in animal models and patients (Arteaga et al. 1992; Parra et al. 2005; García-Rivas and Torre-Amione 2009; Piot et al. 2008). In addition to IR, mPT pore opening was also found to be increased in

Fig. 5 mPT modulation by AGE. **a** Calcium release evoked by AGE is prevented by cyclosporine A (CsA) in isolated mitochondria. **b** Representation of maximal calcium retention from treatments in A. The values are mean±S.D. of 7 separate experiments. **c** Calcium release from mitochondria is promoted by atractyloside (AT). Bongkrekic acid (BKA) blocks ANT preventing the calcium release effect by AT. **d** Representation of maximal calcium retention from treatments in A. *$P \leq 0.05$ vs CSA treatment
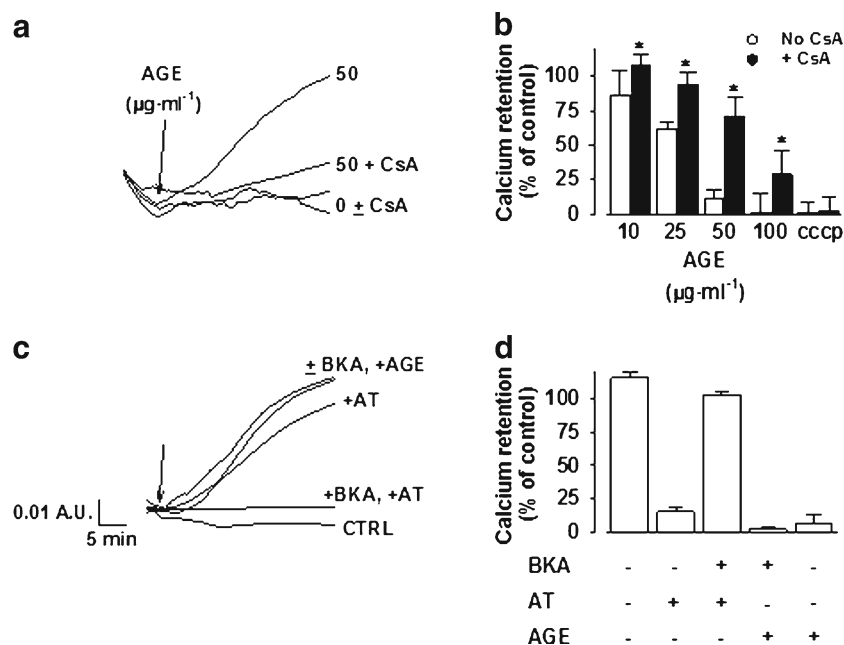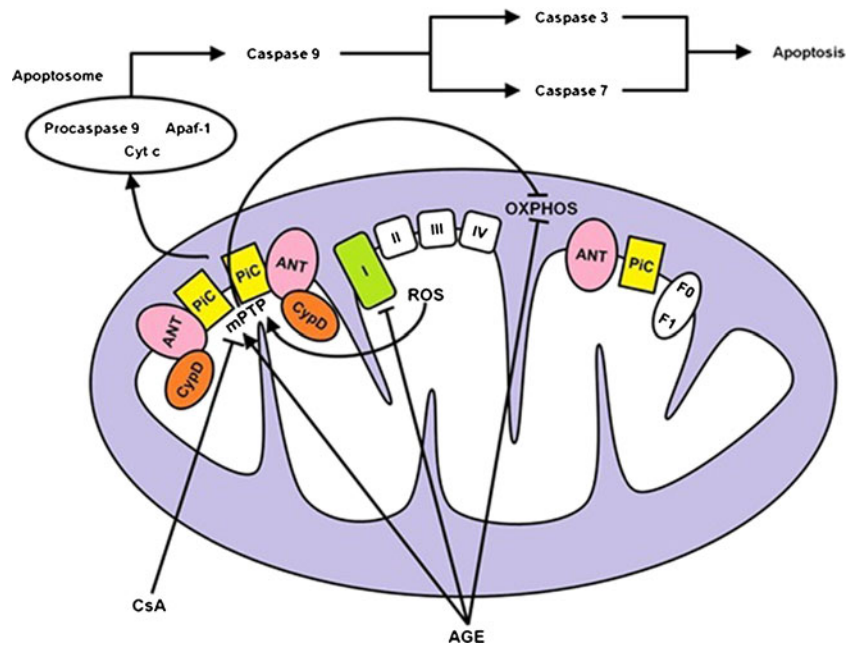
Fig. 6 Model of the mechanisms by which AGE affects mitochondrial function and produces cell death in the cardiac myocyte. AGE inhibits the electron transport chain since it affects primarily the activity of complex I. This, in turn, compromises the proton chemical gradient, diminishes the oxidative phosphorylation, and exacerbates production of ROS. Additionally, AGE showed that in absence of complex I activity, ATP synthesis is also affected by the inhibition of ANT. In these circumstances, AGE is able to promote the permeability transition in the inner membrane of mitochondria and was prevented by CsA, thus involving the opening of mPTP. Release of Cyt c from the intermembranal space to cytoplasm occurs in the mPTP-opened states. The apoptosome is completed with Cyt c, yielding a full activated caspase 9. Apoptosis is in place when caspase 9 activates procaspases 3 and 7

diabetic cardiomyopathy (Oliveira et al. 2003), heart failure (Javadov et al. 2009), neurodegenerative disease (Barsukova et al. 2011) and parkinsonism (Thomas et al. 2011). Interestingly, mPT pore opening was implicated in a similar model to atypical Parkinsonism associated with consumption of AGs (Champy et al. 2003).

To explore the interaction of AGE with the ANT, we determined the mPT pore opening incidence in the presence and absence of the ANT ligand BKA. Figure 5c illustrates the experiment for testing the effects of the known mPT inducer Atractyloside (AT) in the presence and absence of BKA. The results demonstrate that BKA effectively inhibits 90 % of AT-induced mPT pore opening. In contrast, BKA does not inhibit mitochondrial calcium release induced by 50 μg/ml AGE. In panel D, is shown a quantitative analysis of mPT pore opening induced by AGE and ANT blockers. The ANT alternates between two distinct conformations in which adenine nucleotides are either bound to the cytosolic side (c-state) or to the matrix side (m-state) of the IMM. It has been described that the c-conformation is favorable to induce mPT (Brustovetsky and Klingenberg 1996). Carbioxyatractyloside and AT, which bind to ANT in the c-state, activated the mPT pore, whereas BKA, which binds to ANT in the m-state, inhibited the mPT. In accordance to previous reports, our results suggest that AGE does not interact with ANT in the c-state as AT does. Another possibility is that AGE is acting on another structural component of the mPT pore, for example the phosphate carrier (PiC). For instance, Leung et al. 2007 suggested a key role for the PiC in mPT pore formation, by using co-immunoprecipitation experiments to demonstrate CyP-D binding to the PiC (Leung et al. 2008). In this condition, CSA inhibited the opening of mPT pore independent of CAT and BKA modification of ANT.

Conclusions

The mechanism of AGE cardiotoxicity involves mitochondrial dysfunction and activation caspase-dependent apoptosis pathways. The current study demonstrates (1) that AGE affects mechanical performance in the isolated heart, (2) induces cardiomyocytes apoptosis by the mitochondrial pathway signal, (3) inhibits complex I activity, (4) evokes permeability transition through interaction with ANT. The increment in non specific mitochondrial permeability produced by AGE has toxic consequences. This is illustrated in Fig. 6, which represents the mechanisms of mitochondrial damage and how they might induce apoptosis. A better understanding of the mechanisms through which AGE produces cardiotoxicity may uncover novel avenues to avoid side effects in the anti-cancer therapeutics field.

References

Rodriguez-Saona C, Millar J, Trumble J (1998) Isolation, identification, and biological activity of isopersin, a new compound from avocado idioblast oil cells. J Nat Prod 61:1168–1170

Jolad S, Hoffmann J, Schram K, Cole J (1982) Uvaricin, a new antitumor agent from Uvaria accuminata (Annonaceae). J Org Chem 47:3151–3153

Ahammadsahib KI, Hollingworth RM, McGovren JP, Hui YH, McLaughlin JL (1993) Mode of action of bullatacin: a potent antitumor and pesticidal annonaceous acetogenin. Life Sci 53:1113–1120

Degli Esposti M, Ghelli A, Ratta M, Cortes D, Estornell E (1994) Natural substances (acetogenins) from the family Annonaceae are powerful inhibitors of mitochondrial NADH dehydrogenase (Complex I). Biochem J 301(Pt 1):161–167

Morré DJ, de Cabo R, Farley C, Oberlies NH, McLaughlin JL (1995) Mode of action of bullatacin, a potent antitumor acetogenin: inhibition of NADH oxidase activity of HeLa and HL-60, but not liver, plasma membranes. Life Sci 56:343–348

Gustafsson AB, Gottlieb RA (2007) Heart mitochondria: gates of life and death. Cardiovasc Res 77:334–343

Halestrap AP (2009) What is the mitochondrial permeability transition pore? J Mol Cell Cardiol 46:821–831

Liu X, Kim CN, Yang J, Jemmerson R, Wang X (1996) Induction of apoptotic program in cell-free extracts: requirement for dATP and cytochrome c. Cell 86:147–157

Yuan S, Chang H, Chen H, Yeh Y, Kao Y (2003) Annonacin, a mono-tetrahydrofuran acetogenin, arrests cancer cells at the G1 phase and causes cytotoxicity in a Bax- and caspase-3-related pathway. Life Sci 72(25):2853–2861

Oelrichs PB, Ng JC, Seawright AA, Ward A, Schäffeler L, MacLeod JK (1995) Isolation and identification of a compound from avocado (Persea americana) leaves which causes necrosis of the acinar epithelium of the lactating mammary gland and the myocardium. Nat Toxins 3:344–349

Caparros-Lefebvre D, Elbaz A (1999) Possible relation of atypical parkinsonism in the French West Indies with consumption of tropical plants: a case-control study. Caribbean Parkinsonism Study Group. Lancet 354:281–286

Champy P, Höglinger GU, Féger J, Gleye C, Hocquemiller R, Laurens A et al (2003) Annonacin, a lipophilic inhibitor of mitochondrial complex I, induces nigral and striatal neurodegeneration in rats: possible relevance for atypical parkinsonism in Guadeloupe. J Neurochem 88:63–69

Escobar-Khondiker M, Hollerhage M, Muriel MP, Champy P, Bach A, Depienne C et al (2007) Annonacin, a natural mitochondrial complex I inhibitor, causes tau pathology in cultured neurons. J Neurosci 27:7827–7837

Neubauer S (2007) The failing heart—an engine out of fuel—N Engl J Med 15;356(11):1140–1151

Yang H, Li X, Tang Y, Zhang N, Chen J, Cai B (2009) Supercritical fluid CO2 extraction and simultaneous determination of eight annonaceous acetogenins in Annona genus plant seeds by HPLC-DAD method. J Pharm Biomed Anal 49:140–144

De Jesús García-Rivas G, Guerrero-Hernández A, Guerrero-Serna G, Rodríguez-Zavala JS, Zazueta C (2005) Inhibition of the mitochondrial calcium uniporter by the oxo-bridged dinuclear ruthenium amine complex (Ru360) prevents from irreversible injury in postischemic rat heart. FEBS J 272:3477–3488

Wolska BM, Solaro RJ (1996) Method for isolation of adult mouse cardiac myocytes for studies of contraction and microfluorimetry. Am J Physiol 271:H1250–H1255

de Garcia-Rivas GJ, Carvajal K, Correa F, Zazueta C (2006) Ru360 a specific mitochondrial calcium uptake inhibitor, improves cardiac post-ischaemic functional recovery in rats in vivo. Br J Pharmacol 149:829–837

Waldmeier P, Feldtrauer J, Qian T (2002) Inhibition of the mitochondrial permeability transition by the nonimmunosuppressive cyclosporin derivative NIM811. Mol Pharmacol 62(1):22–29

Chávez E, García N, Zazueta C, Correa F (2003) The composition of the incubation medium influences the sensitivity of mitochondrial permeability transition to cyclosporin A. J Bioenerg Biomembr 35 (2):149–156

Ortega R, Garcia N (2009) The flavonoid quercetin induces changes in mitochondrial permeability by inhibiting adenine nucleotide translocase. J Bioenerg Biomembr. Volume 41, Number 1

Bulteau A-L, Lundberg KC, Ikeda-Saito M, Isaya G, Szweda LI (2005) Reversible redox-dependent modulation of mitochondrial aconitase and proteolytic activity during in vivo cardiac ischemia/reperfusion. Proc Natl Acad Sci USA 102:5987–5991

Ohkawa H, Ohishi N, Yagi K (1979) Assay for lipid peroxides in animal tissues by thiobarbituric acid reaction. Anal Biochem 95:351–358

Burger W, Naudé T, van Rensburg I, Botha C, Pienaar A (1993) Cardiomyopathy in ostriches (Struthio camelus) due to avocado (Persea americana var. guatemalensis) intoxication. J S Afr Vet Assoc 65(3):113–118

Butt AJ, Roberts CG, Seawright AA, Oelrichs PB, Macleod JK, Liaw TY, et al. (2006) A novel plant toxin, persin, with in vivo activity in the mammary gland, induces Bim-dependent apoptosis in human breast cancer cells. Mol Cancer Ther 5:2300–2309

Lee Y, Gustafsson ÅB (2009) Role of apoptosis in cardiovascular disease. Apoptosis 14:536–548

Roberts CG, Gurisik E, Biden TJ, Sutherland RL, Butt AJ (2007) Synergistic cytotoxicity between tamoxifen and the plant toxin persin in human breast cancer cells is dependent on Bim expression and mediated by modulation of ceramide metabolism. Mol Cancer Ther 6:2777–2785

Murai M, Ichimaru N, Abe M, Nishioka T, Miyoshi H (2006) Mode of inhibitory action of Δlac-acetogenins, a new class of inhibitors of bovine heart mitochondrial complex I. Biochemistry 45:9778–9787

Alvarez Colom O, Neske A, Chahboune N, Zafra-Polo MC, Bardón A (2009) Tucupentol, a novel mono-tetrahydrofuranic acetogenin from Annona montana, as a potent inhibitor of mitochondrial complex I. Chem Biodivers 6:335–340

Pastorino JG, Wilhelm TJ, Glascott PA, Kocsis JJ, Farber JL (1995) Dexamethasone induces resistance to the lethal consequences of electron transport inhibition in cultured hepatocytes. Arch Biochem Biophys 318:175–181

Wolvetang EJ, Johnson KL, Krauer K, Ralph SJ, Linnane AW (1994) Mitochondrial respiratory chain inhibitors induce apoptosis. FEBS Lett 339:40–44

Isenberg JS, Klaunig JE (2000) Role of the mitochondrial membrane permeability transition (MPT) in rotenone-induced apoptosis in liver cells. Toxicol Sci 53:340–351

Terada H (1981) The interaction of highly active uncouplers with mitochondria. Biochim Biophys Acta 639:225–242

de Graaf AO, van den Heuvel LP, Dijkman HBPM, de Abreu RA, Birkenkamp KU, de Witte T et al (2004) Bcl-2 prevents loss of mitochondria in CCCP-induced apoptosis. Exp Cell Res 299:533–540

Castilho RF, Meinicke AR, Almeida AM, Hermes-Lima M, Vercesi AE (1994) Oxidative damage of mitochondria induced by Fe(II)citrate is potentiated by Ca2+ and includes lipid peroxidation and alterations in membrane proteins. Arch Biochem Biophys 308:158–163

McStay GP, Clarke SJ, Halestrap AP (2002) Role of critical thiol groups on the matrix surface of the adenine nucleotide translocase in the mechanism of the mitochondrial permeability transition pore. Biochem J 367:541–548

Crompton M, Virji S, Ward JM (1998) Cyclophilin-D binds strongly to complexes of the voltage-dependent anion channel and the adenine nucleotide translocase to form the permeability transition pore. Eur J Biochem 258:729–735

Bernardi P (1992) Modulation of the mitochondrial cyclosporin A-sensitive permeability transition pore by the proton electrochemical gradient. Evidence that the pore can be opened by membrane depolarization. J Biol Chem 267:8834–8839

Vercesi AE (1987) The participation of NADP, the transmembrane potential and the energy-linked NAD(P) transhydrogenase in the process of Ca2+ efflux from rat liver mitochondria. Arch Biochem Biophys 252:171–178

Arteaga D, Odor A, López RM, Contreras G, Pichardo J, García E et al (1992) Impairment by cyclosporin A of reperfusion-induced arrhythmias. Life Sci 51:1127–1134

Parra E, Cruz D, García G, Zazueta C, Correa F, García N et al (2005) Myocardial protective effect of octylguanidine against the damage induced by ischemia reperfusion in rat heart. Mol Cell Biochem 269:19–26

García-Rivas GJ, Torre-Amione G (2009) Abnormal mitochondrial function during ischemia reperfusion provides targets for pharmacological therapy. Methodist Debakey Cardiovasc J 5, 2–7

Piot C, Croisille P, Staat P, Thibault H, Rioufol G, Mewton N et al (2008) Effect of cyclosporine on reperfusion injury in acute myocardial infarction. N Engl J Med 359:473–481

Oliveira PJ, Seiça R, Coxito PM, Rolo AP, Palmeira CM, Santos MS et al (2003) Enhanced permeability transition explains the reduced calcium uptake in cardiac mitochondria from streptozotocin-induced diabetic rats. FEBS Lett 554:511–514

Javadov S, Rajapurohitam V, Kilić A, Zeidan A, Choi A, Karmazyn M (2009) Anti-hypertrophic effect of NHE-1 inhibition involves GSK-3β-dependent attenuation of mitochondrial dysfunction. J Mol Cell Cardiol 46:998–1007

Barsukova AG, Bourdette D, Forte M (2011) Mitochondrial calcium and its regulation in neurodegeneration induced by oxidative stress. Eur J Neurosci 34:437–447

Thomas B, Banerjee R, Starkova NN, Zhang SF, Calingasan NY, Yang L et al (2011) Mitochondrial permeability transition pore component cyclophilin D distinguishes nigrostriatal dopaminergic death paradigms in the MPTP mouse model of Parkinson's disease. Antioxid Redox Signal. doi:10.1089/ars.2010.3849

Brustovetsky N, Klingenberg M (1996) Mitochondrial ADP/ATP carrier can be reversibly converted into a large channel by Ca2. Biochemistry 35:8483–8488

Leung AWC, Varanyuwatana P, Halestrap AP (2008) The mitochondrial phosphate carrier interacts with cyclophilin D and may play a key role in the permeability transition. J Biol Chem 283:26312–26323